ROMANIAN JOURNAL OF INFORMATION SCIENCE AND TECHNOLOGY
Volume **10**, Number 1, 2007, 97–111

Investigation of Silver-, Meso- and Nanoporous Silicon Composite Layers for Biomedical Applications

I. KLEPS[1], M. MIU[1], M. DANILA[1], M. SIMION[1],
T. IGNAT[1], A. BRAGARU[1], L. DUMITRU[2], G. TEODOSIU[2]

[1]National Institute for Research and Development in Microtechnologies (IMT-Bucharest), P.O. Box 38-160, Bucharest, Romania
E-mail: irinak@imt.ro

[2]Institute of Biology,
296 Splaiul Independenţei, P.O. Box 56-53, Bucharest, 060031, Romania
E-mail: biologie@ibiol.ro

Abstract. The study of the porous silicon (PS) structures is important for both fundamental understanding of nano-systems as well for its possible applications. In this paper various Ag/PS based composite layers were experimented in order to enlarge the PS applications, especially in biomedical field. The Ag nanoparticles/silicon nanocomposite layers as-deposited and thermal treated were investigated by optical microscopy, X-ray diffraction, and biological tests. Ag/PS layers can be used as a composite matrix for microelement delivery with application in homeopathy. On the other hand Ag nanoparticles on nanocrystalline Si are important for their anti-microbial properties. In minute concentrations, Ag is highly toxic to germs while relatively non-toxic to human cells. Microbes are unlikely to develop a resistance against silver, as they do against conventional and highly targeted antibiotics. The experimental results sustain the Ag/Si nanocomposite structures as anti-microbial matrix.

1. Introduction

Porous silicon (PS) layers formed on the crystalline Si substrates by electrochemical etching have been known from many years, due to its particular optical properties

[1] and have recently attracted attention due to its biocompatible nature [2]. Porous silicon is obtained by partial electrochemical dissolution in hydrofluoric acid based solutions; depending on the etching conditions, porous silicon has a complex, anisotropic nanocrystalline architecture of high surface area [3–4]. In this paper various Ag-PS composite layers were experimented in order to enlarge the PS applications, especially in biomedical field.

The porous silicon composite layers are of particular relevance for bioimplant applications: they can be used as a composite matrix for microelement delivery [5–6] or for cell adhesion, or as active part of DNA analyses microdevices [7–9]. Small amount of silver nanoparticles are non-toxic for human body and it is extensively used in homeopathy. On the other hand, Ag nanoparticles on nanocrystalline Si are important for their anti-microbial properties. In very low concentrations, Ag is highly toxic to germs while relatively non-toxic to human cells. Microbes are unlikely to develop a resistance against silver, as they do against conventional and highly targeted antibiotics. Morphological, structural and chemical properties as well as biological investigations such as bioresorbability or antibactericide properties of these composite layers were investigated.

2. Ag-Mesoporous silicon layers for silver controlled delivery

2.1. Experimental conditions for mesoporous silicon matrix fabrication

In order to obtain an Ag-PS matrix with silver diffused in silicon pores and fibrils for biological applications, different materials in a variety of preparation conditions have been used for the impregnation process.

The starting material is crystalline n-Si wafers (100) oriented and with 3–5 Ω·cm resistivity. The PS layers were performed by an electrochemical process, in the ethanoic HF solution, 20% at 100 mA/cm^2 current density and 5 minutes. The porosity of PS layer used in these experiments determined by gravimetric measurements was 30%. The PS layer thickness of 30 μm was measured by cross section scanning electron microscopy (SEM), as can be seen in the Figs. 1 and 2. The pores are hundred nanometers wide, cylindrically shaped, straighter and good defined.

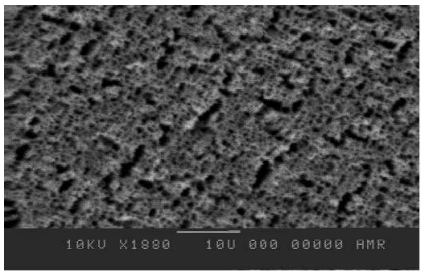

Fig. 1. Top view SEM image for mesoporous PS/Si-n

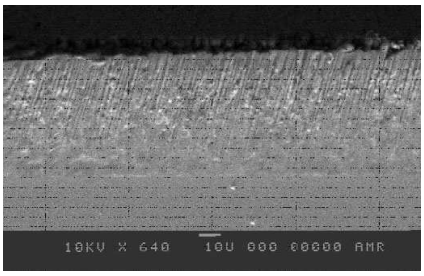

Fig. 2. Cross-section SEM image for mesoporous PS/Si-n

2.2. Experimental conditions for Ag impregnation on mesoporous silicon

In order to achieve the mesoporous silicon impregnation with silver we used $AgNO_3$ solution. For silver impregnation the following procedure was applied: (i) spin-on of AgNO3 solution on PS surface; (ii) treatment at 47°C, in a H_2:N_2 atm., for 1 hour; (iii) a melting process at 250°C, H_2:N_2 atm., 1h; (iv) a diffusion process, at 450°C, in a H_2:N_2 atm., for 1h.

The chemical behavior of PS as a moderate reducing agent for silver ions is described by the following reactions [9]:

$$Ag^+ + 2\ \text{Si-H (from the PS surface)} \longrightarrow Ag + 2H_2 + 2Si + H^+$$

In presence of water traces from the furnace, the reaction is:

$$Ag^+ + Si\ (\text{surface}) + 2H_2O \longrightarrow Ag + H_2 + SiO_2 + 2H^+$$

2.3. Morphological and structural characterization of Ag-meso-PS composite layers

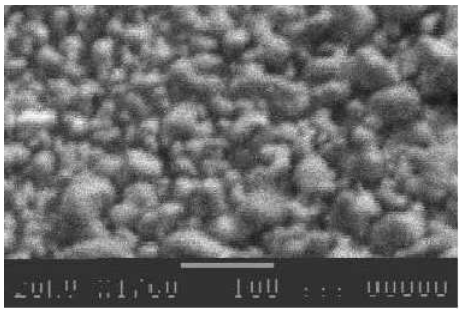

Fig. 3. SEM image of the Ag/PS/Si-n structure.

A SEM image of the Ag/PS/Si-n as-deposited structure is presented in Fig. 3, and some SEM images of the mesoPS surface after the impregnation with silver, in Fig. 4.

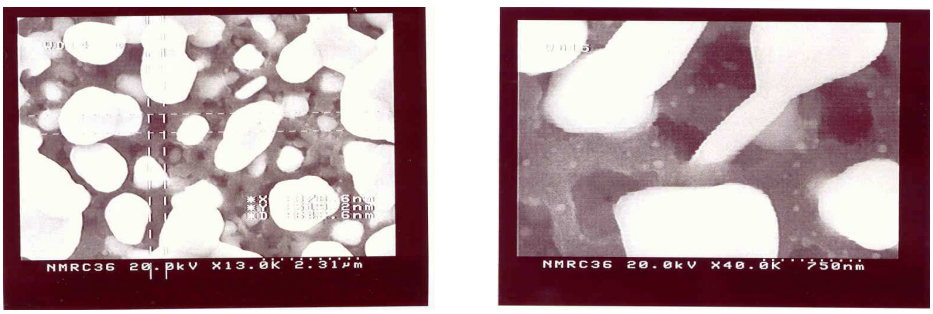

Fig. 4. SEM images of the test structures: (a) after treatment at 47°C, in a H2:N2 atm., for 1 hour; (b) after silver diffusion in pores.

Some Ag clusters with diameters around 2 μm on PS surface can be observed – Fig. 4a and, also, pores filled with silver – Fig. 4b.

A cross section - SEM image, of the PS layer filled with silver it can be observed in Fig. 5.

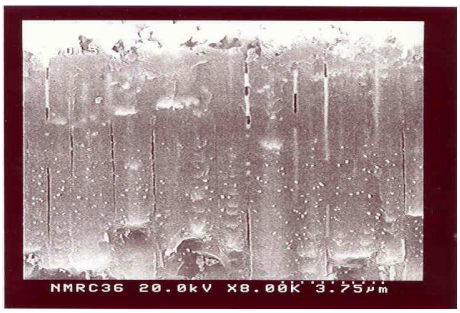

Fig. 5. SEM image of the PS layer.

In this image you can see the diffusion of the silver particles into the porous structure. In order to have a quantitative analysis of the metal amount inside the porous structure, we used the EDX spectroscopy method (Energy Dispersive X-Ray Spectroscopy) – Fig. 6.

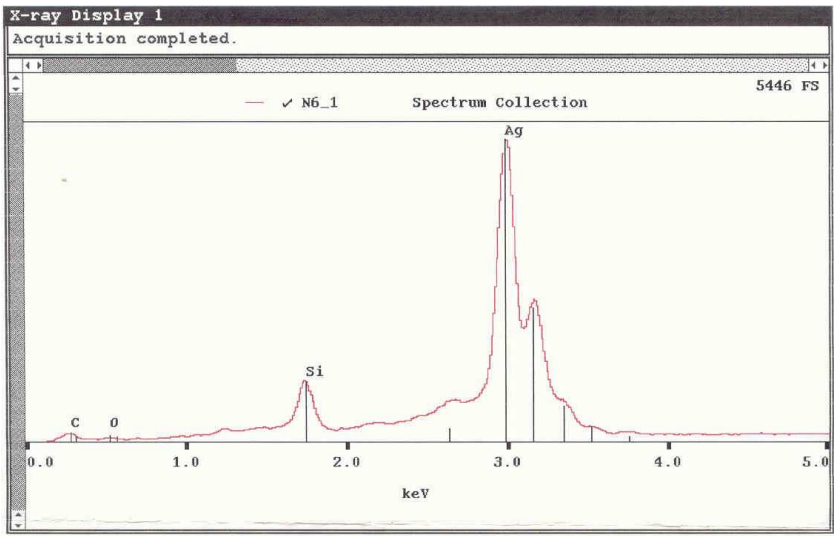

Fig. 6. EDX spectrum after silver diffusion inside the PS.

From this spectrum it can be seen a bigger amount of Ag inside the PS layer, bigger then silicon atoms. For new results regarding chemical structure of the metallic compounds formed on PS surface we used UV–VIS spectroscopy measurements.

In Fig. 7, are presented, comparatively, UV–VIS absorption specters corresponding to the PS structures, before and after impregnation process.

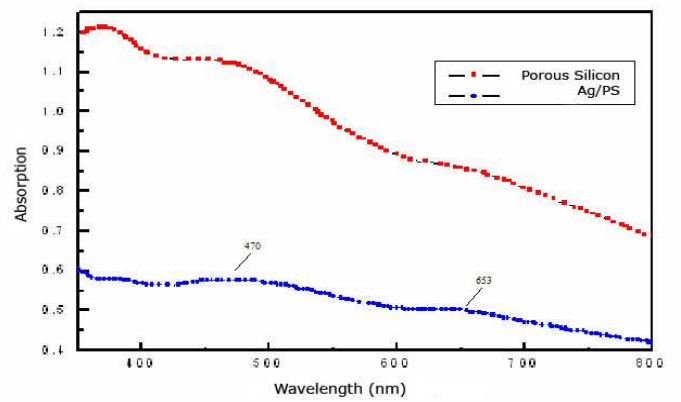

Fig. 7. UV–VIS absorption spectres corresponding to PS structures after silver diffusion.

In the case of $AgNO_3$, after diffusion process, the deposited silver is metallic silver and the low VIS absorption bands cannot be attributed to the silver because of the d^{10} orbital that is full completed and cannot be attributed to the d-d (d^{10} s^1p^0) transitions.

These can be considered bands for PS and, on the silver deposited surface the intensity of the band is low and it's moving. It's about the band corresponding to 470 nm (21.276 cm^{-1}) which will become low in the moment of the silver deposition and it's moving to 20.576 cm^{-1}. The same thing it's happening in the case of band for 653 nm (15.313 cm^{-1}) which is lower in the silver deposition field and it's moving to 15.151 cm^{-1}. Finally, we can say that reaction product is metallic silver and the PS surface with deposited silver it's changing the optical properties.

2.4. Bioresorbable properties

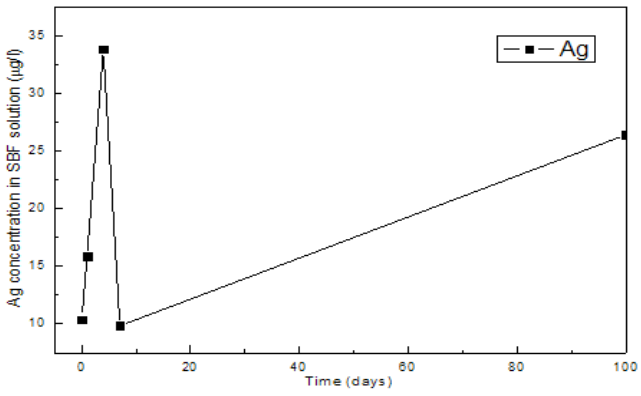

Fig. 8. Ag release and PS matrix degradation in SBF solution.

In the first three days a strong Ag release was observed due to the dissolution of the silver salt from the PS pores (Fig. 8). After that, the silver release takes place in the same time with the degradation of the PS matrix in SBF solution. A higher silver concentration in depth of PS skeleton was observed.

3. Silver/porous silicon (PS) nanocomposite layers with antibactericide properties

Medical microdevice manufacturers need to prevent biofilm formation, which allows the micro-organisms to adhere to any surface, living or nonliving. It was demonstrated that silver is able to disrupt the critical functions in a microorganism [10]. For example, it has a high affinity for negatively charged side groups on biological molecules, such as sulfhidryl, carboxyl, phosphate, and other charged groups distributed throughout microbial cells [11]. Silver is also more efficient than traditional antibiotics because it is extremely active in small quantities; for certain bacteria, as little as one part per billion of silver may be effective in preventing cell growth.

Surface-application chemistries vary, but they are usually designed to deposit either metallic silver or an ionic salt of silver to the medical device surface. The limitation of ionic salts is that they are only active for a short period of time – often only for a few days. By contrast, metallic silver nanoparticles persist in delivering antimicrobial silver for as long as 100–200 days; in this context, one method under investigation is to incorporate Ag nanoparticles with antimicrobial properties into the microdevices themselves [12].

The aim of this study is to investigate Ag/PS antibactericide properties for biosensors and implantable microdevice applications.

3.1. Experimental procedure

The nanostructured silicon (PS) layers, used as support in the experiments for Ag/Si nanocomposite structures, were obtained by electrochemical etching of Si wafers: Si (100), p^+ type, 5 mΩ·cm resistivity. Determined by gravimetric measurements, the porosity of PS layers used in these experiments was 38% and the corresponding pores have 5 nm diameter.

In order to compare the bactericide effect, different methods were used to fabricate Ag / porous silicon layers: (i) physical vapor deposition (PVD) of thin Ag layers – 100 nm thicknesses; (ii) immersion in $AgNO_3$ salt solution, saturated and 1% diluted in ethanol, respectively. The Ag/PS/Si nanocomposites layers were obtained after an additional thermal treatment (T.T.) in reducing atmosphere (H_2 and N_2) at 500°C and 900°C.

The Ag melting point is 960°C, while Ag_2O is 200°C and $AgNO_3$ melting point is 212°C; Ag on PS surface is partially oxidized, and it is expected that during thermal treatment the Ag_2O and $AgNO_3$ to be melt and to fill partially the PS pores. The smaller the particle size, and the greater the ratio of surface area to volume will give a greater the area available for oxidation.

The experimental conditions related to the sample preparation are presented in Table 1:

Table 1. Experimental data

PS / Si (fabr. cond.)	**PVD-Ag**	**$AgNO_3$ salt**	**T.T.** [°C]
– 25% HF conc.;	*RX4*		as-dep.
– time: 30min;	*RX5*	*RX1* (1% $AgNO_3$ sol.) *RX2* ($AgNO_3$ sat. sol.)	500
– current density: 3 mA/cm^2;	*RX6*		900

3.2. Silver/si nanocomposite layers characteristics

Ag/PS sample morphology was investigated by optical (Fig. 9 a–d) and by fluorescence microscopy (Fig. 10).

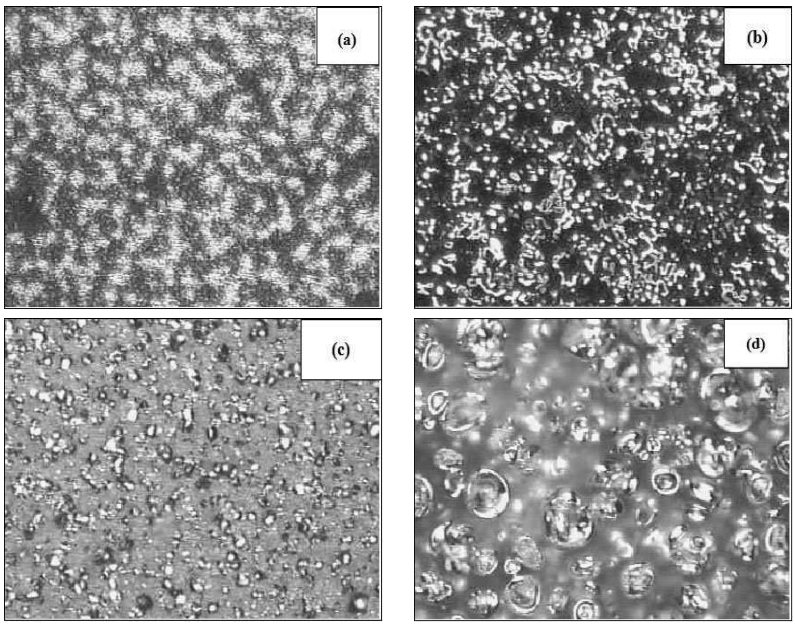

Fig. 9. Optical images of Ag/PS composite layers:
(a) PVD-Ag/PS 500°C; ×20; (b) PVD-Ag/PS 900°C; ×20;
(c) Ag (sol.dil.)/PS, 500°C; ×20; (d) Ag (sat.sat.)/PS, 900°C; ×20.

The optical analyses reveal modifications of Ag particles deposited by PVD on the PS surface, after thermal treatment at 500°C and 900°C due to their partial oxidation – Fig. 9 (a) and (b). A low number of small particles from $AgNO_3$ 1% diluted solution after thermal treatment at 500°C is observed – Fig. 9 (c), and their nucleation process after 900°C treatment – Fig. 9 (d). It is observed that all Ag/PS samples excepting $AgNO_3$ thick layers on PS, are not continuous, and have different morphologies.

Fluorescence of the Ag/PS composite layers was investigated by reflexion – fluorescence microscope type.

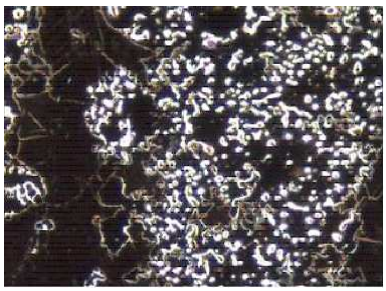

Fig. 10. Image obtained by fluorescence microscope – Ag/PS 500°C (×20).

The crystalline structure of the nanocomposite layers was investigated by X-ray diffraction method (WAXD) [13], using a DRON-3 diffractometer in θ-2θ angular scanning configuration using a Co X-ray tube (X-ray K_α wavelength of $\lambda_{K_{\alpha_1}} = 1.789007$ Å). The operating power was U = 35 kV, I = 20 mA, with a 2θ step of 0.02° and an integration time of 10 s. The continuous X-ray emission spectrum of the X-ray tube was filtered using a Fe filter (the Co K_β and lower wavelength radiations are reduced by more than an order of magnitude, Fig. 11).

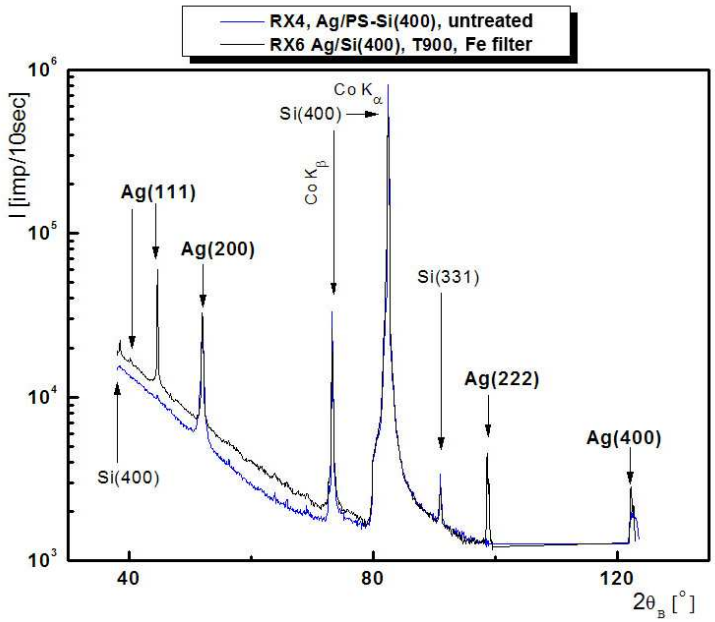

Fig. 11. The continuous X-ray emission spectra of the X-ray tube using a Fe filter.

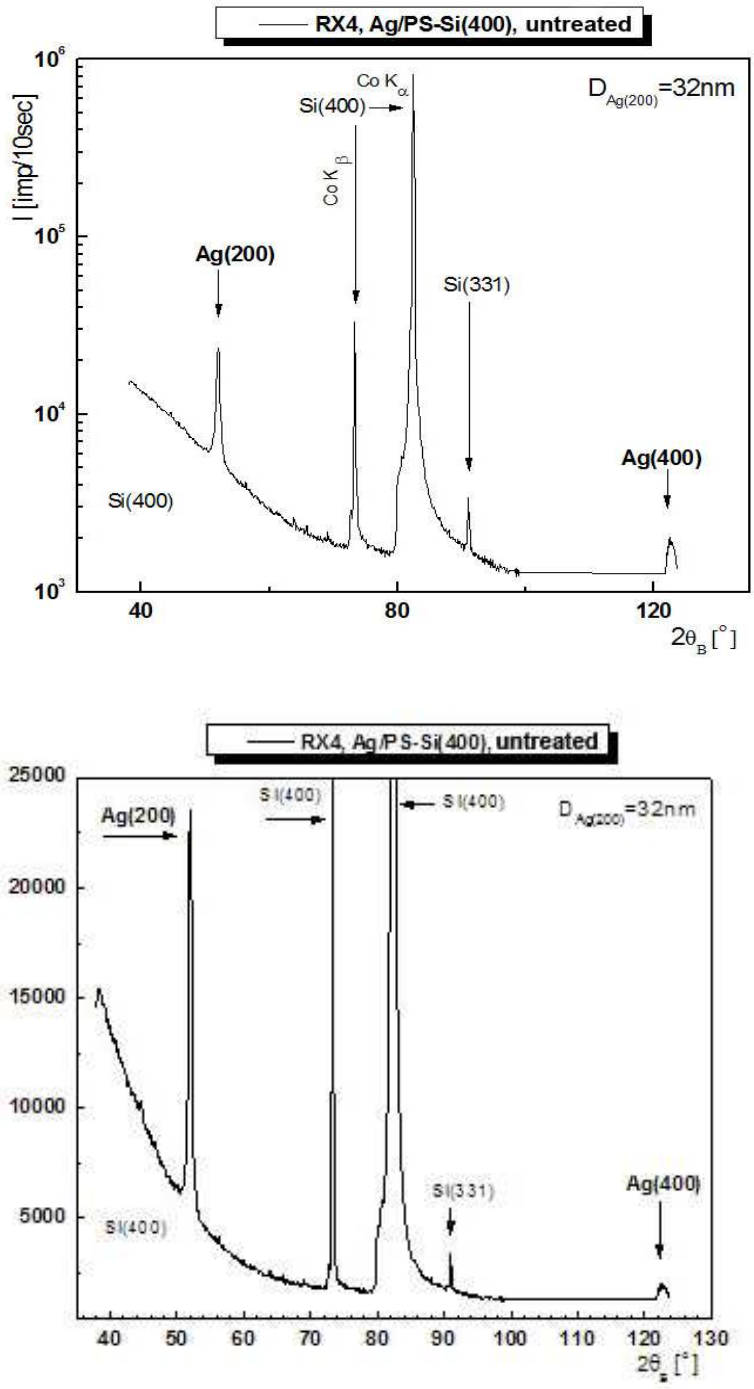

Fig. 12. X-ray spectra of the as-deposited Ag/PS/Si(400).

The diffraction spectra of the as-deposited Ag films on PS (Fig. 12) reveal a strong (220) texture of the FCC nanocrystalline Ag phase. The grain size of the as-deposited Ag film on PS calculated with the Scherrer equation: $D_{hkl} = \frac{K \cdot \lambda}{\beta \cdot \cos\theta_B}$ is D_{220} = 32 nm, where K is a constant approximately equal to unity (0,9), λ is the X-ray wavelength (Co K$_\beta$), and θ_B is the Bragg scattering angle. A distinctive feature of the X-ray spectra of the as-deposited Ag film on PS is the (331) Si diffraction line. The presence of this diffraction line, connected with the very high and sharp diffraction line of the substrate [Si(400)] point to the presence of moderate strain fields in the porous silicon substrate layer. The monocrystalline nature of the porous silicon substrate implies the presence of only one X-ray diffraction line, that of the Si (400) substrate. Moreover, knowing that the (331) atomic plane of the FCC Si phase makes an angle of 46.5° with the (400) plane (the Bragg angle $\theta_{BSi(400)}$ = 41.24°, $\theta_{BSi(331)}$ = 45.88° – Co Kα), one can easily calculate the medium tilt angle of the porous silicon matrix induced by the crystallization of Ag films inside the (nano)pores, i.e ϕ= 46.5°. Thus the induced strain fields are not sufficient to produce the cracking and amorphisation of the PS layer, but are high enough just to produce a tilt of the crystalline atomic matrix of the PS (400) oriented substrate.

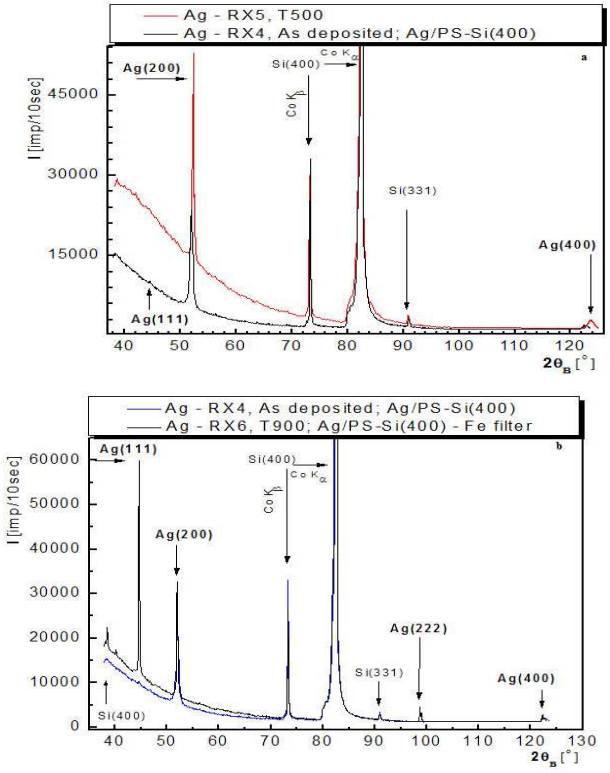

Fig. 13. X-ray diffraction patterns of Ag/PS for as-deposited and after thermal annealing at 500°C and 900°C.

The variation of the structural characteristics of the silver deposited on Si nanostructured layers as a function of temperature annealing were investigated comparatively to as-deposited samples – Fig. 13.

From the point of view of the microstructure analysis of the Ag films on PS, the annealing treatment at 500°C has small effect (crystallization continue on (200) planes, and the films have a higher crystalline content), while annealing at 900°C produces a mixed (111) and (200) texture, with bigger grain sizes. The Ag films deposited from diluted solution of $AgNO_3$ are in an initial stage of crystallisation, with a high amorphous content, deduced from the large amorphous hump centred at 44.5° and from the high background and very low intensities of the corresponding Ag diffracting planes – Fig. 14.

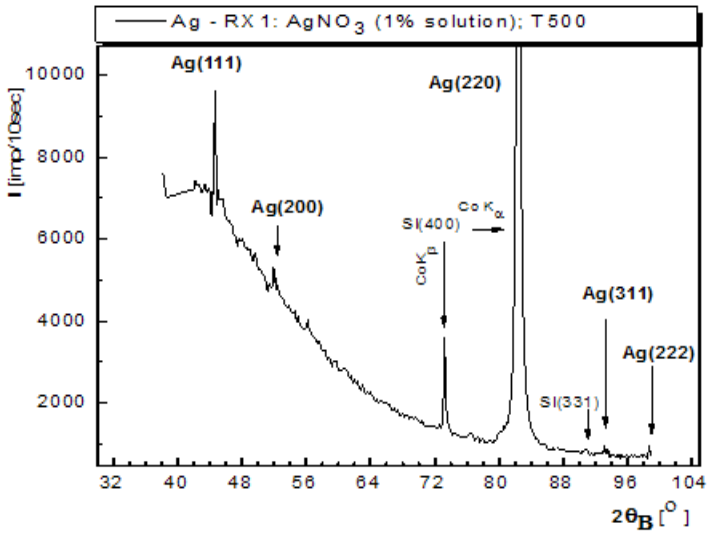

Fig. 14. X-ray diffraction pattern for $AgNO_3$ (1% solution) / PS samples after thermal annealing at 500°C.

This fact can be explained by the low content of Ag atoms on the surface, and thus by the resulting lower thickness of the deposited Ag crystalline layer. Although the total thickness of the layer may be bigger than in the case of the samples Ag-RX4 – Ag-RX6 (the diffracted intensity from the (400) Si is lower), the crystalline content is very low (very weak diffracted intensities from Ag atomic planes). The films deposited from salt are the thickest and with the lowest crystalline content. Deposition from concentrated solution of $AgNO_3$ produces Ag films with a high and predominant (111) texture and a grain size of 60–72 nm, with a crystalline content higher than in the case of RX1 sample from diluted solution.

The diffracted intensities from the substrate planes - Si (440) is the lowest in this sample group, revealing either thicker film or/and incomplete crystallisation. The films deposited from salt are the thickest, but the crystalline content is the lowest.

3.3. Ag/PS antibactericide properties

In order to investigate the antibactericide properties of the Ag/PS structures a heterotrophic bacterium isolated from natural aquatic habitat, characterized as Gram-positive, rod-shaped, endospore-forming bacteria, from Bacillus genus was used. A specific protocol was applied, as follows: microorganisms were grown on a solid medium represented by nutrient agar slant. Cultures were incubated at 30°C, for 24 hours. After this period, the microorganisms in the exponential growth phase were inoculated in nutrient broth, in Erlenmeyer flasks. For each culture a preinoculum on liquid medium was performed, which was afterwards used at a 1/10 rate to initiated new cultures. Cultures were incubated at 30°C, under continuous stirring (200 rpm), in darkness. From these cultures were performed subcultures at which were added plates of porous silicon. The subcultures were incubated in static conditions, at 30°C. The growth of microorganisms was monitorized during of 76 hours (Table 2), by spectrophotometric determination of cellular density (O.D.) at 660 nm, compared with a blank one (uninoculated liquid medium).

Table 2.

No.	Sample	Cellular growth (O. D. 660 nm)			
		T_0	24 h	48 h	76 h
1	Ag/PS salt	0.787	1.428	1.451	1.411
2	Ag/PS 900°C	0.731	1.192	1.205	1.239
3	Ag/PS 500°C	0.797	1.239	1.240	1.218
4	Ag/PS dil. sol.	0.767	1.295	1.329	1.293
5	Ag/PS as-prep	0.767	1.275	1.231	1.421
6	PS	0.776	1.546	1.557	1.629

The results obtained show the ability of the strain to grow in presence of porous silicon plates, in all experimental variants.

The evolution of cellular growth is presented in Fig. 15:

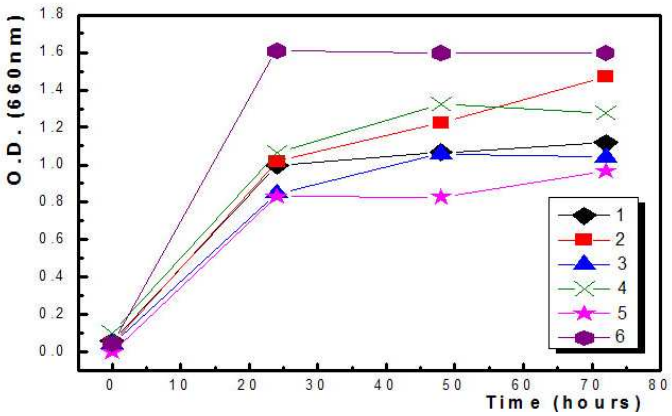

Fig. 15. The growth evolution of P 1/1 strain in presence of porous silicon plates.

The maximal growth was recorded in the case of sample 6 represented by untreated porous silicon plates. The value obtained in this variant (1.629 U.O.D.) was higher to that obtained in bacterial culture without porous silicon (1.392 U.O.D.).

In the second experiments, the plates of porous silicon were taken out from the cultures and were immersed in sterile conditions, in flaks with sterile culture media and were incubated in static conditions, at 30°C, for 72 hours. The results of microorganisms' growth studies are presented in Table 3.

Table 3.

No.	Sample	Cellular growth (O.D. 660 nm)		
		24 h	48 h	72 h
1	Ag NO_3 salt/PS	0.862	0.931	0.981
2	Ag/PS 900°C	0.885	1.088	1.336
3	Ag/PS 500°C	0.711	0.924	0.904
4	$AgNO_3$/PS diluted solution	0.931	1.186	1.142
5	Ag/PS untreated	0.696	0.693	0.831
6	PS	1.474	1.462	1.464

The maximal growth was recorded in the sample 6 represented by untreated PS plates (1.464 U.D.O) and the evolution of cellular growth is presented in Fig. 16:

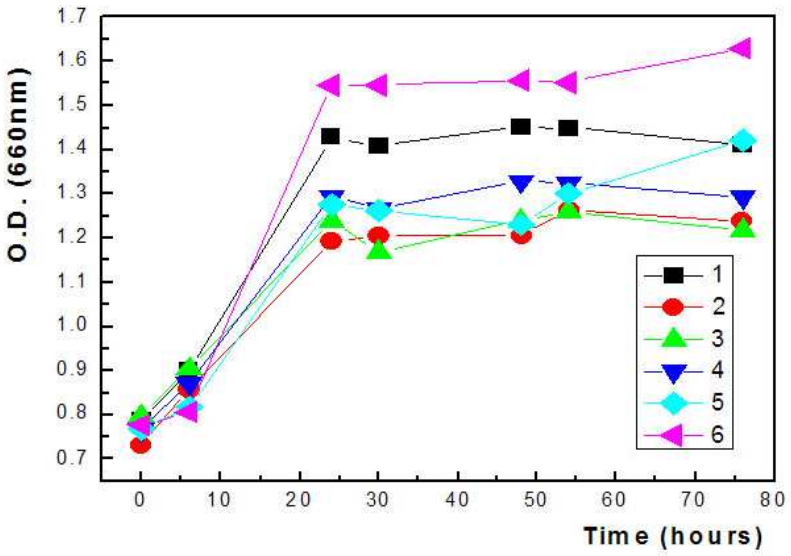

Fig. 16. The growth evolution of bacterial cells from PS plates.

The growth of strain used in experiments was determinate also in the samples with silver (variants 1–5), where the cellular densities obtained were between 0.831 U.D.O. (Ag / PS untreated) and 1.336 U.D.O. (Ag / PS 900°C). This result indicated that the cellular growth was not inhibited by presence of silver from medium, but it is lower.

The results obtained in the second experiment shown the ability of bacterial cells to be attached to porous silicon plates and initiate new cultures in sterile growth medium. In both experiments the microorganisms recorded in the case of all Ag/PS nanocomposite samples were lower compared with samples with PS without Ag.

4. Conclusions

PS is a very suitable material for composite layer preparation because it offers a surface topography controllable with nm resolution in three dimensions and allows chemical surface modifications. The structure of the PS composite layers strongly depends on the following parameters: PS initial porosity, method used for filling the PS pores and subsequently treatments. Generally these parameters were adjusted depending on application. Different PS composite layers were realized for silver release or as biocompatible support with antibactericide properties.

Silver particles morphology was investigated by optical and fluorescence microscopies and the crystalline structure of the Ag films were investigated by X-ray diffraction methods. The annealing treatment at T = 500°C has no effect from the point of view of the microstructure analysis of the Ag films on PS (crystallization continues on (200) planes, 200 the films have a higher crystalline content), while annealing at 900°C produces a mixed (111) and (200) texture, with bigger grain sizes.

Two experiments were performed to investigate the antibactericide properties of the Ag/PS structures. The maximal growth of microorganisms was recorded in the case of sample 6 represented by untreated porous silicon plates without silver. We observe that although metallic silver has no antimicrobial properties, by oxidation results the ionic form which is active. The Ag/Si nanocomposite layers realisated by the proposed thermally treatments allow the oxidation reaction to occur at the surface of the Ag particle when it is exposed to moisture such as body fluids. Silver metal oxidizes very slowly, however, so it persists on the device to extend its usefulness.

The experimental results sustain the Ag/Si nanocomposite structures as antimicrobial matrix.

Acknowledgements. This work was part of the national CEEX program, Contract no. 67/2005 and Contract no. 42/2005.

References

[1] CULLIS, A. G., CANHAM, L. T., WILLIAMS, G. M., SMITH, P. W., DOSSER, O. D., J. Appl. Phys., **75**(1), p. 493, 01 Jan 1994.

[2] CANHAM, L., *U. S. Patent*, 6 322 895, 2001.

[3] CANHAM, L., et al., international patent WO 99/53898, 1999.

[4] MIU, M., ANGELESCU, A., KLEPS, I., SIMION, M., BRAGARU, A., NEGHINA, T., MODREANU, M., IACOPINO, D., ROSEINGRAVE, P., *Porous silicon matrix as mineral microreservoir*, *CAS*, 28.09–2.10, Sinaia, 2003.

[5] CARSTENSEN, J., CHRISTOPHERSEN, M., FOLL, H., Solid State Letters, **2**(3), 1999, p. 126.

[6] KLEPS, I., ANGELESCU, A., MIU, M., SIMION, M., AVRAM, M., BRAGARU, A., *Silicon etching processes for nanostructure fabrication*, 4th EC/NSF Workshop on Nanotechnology: Tools and Instruments for Research and Manufacturing, 12–13 June 2002, Grenoble, France.

[7] INOKUMA, T., et al, J. Appl. Phys., **83** (4) 1998, pp. 2228–2234.

[8] UMEZU, I., et al, J. Non-Crystalline Solids, **266–269**, 2000, pp. 1029–1032.

[9] FAUCHET, M., in D. J. Lockwood (Ed.), *Semiconductors and Semimetals*, vol. **49**, Academic Press, San Diego, 1998, p. 206.

[10] TOBLER, D., WARNER, L., *Nanotech Silver Fights Microbes in Medical Devices*, Med. Dev. & Diag. Ind., **27**, no. 5, 2005, p. 164;

[11] FU-REN, F., BARD, A., J. Phys. Chem., **106**, 2002, p. 279.

[12] TOBLER, D., WARNER, L., *Nanotech Silver Fights Microbes in Medical Devices*, Med. Dev. & Diag. Ind., **27**, no. 5, 2005, pp. 164–169.

[13] KLEPS, I., DANILA, M., ANGELESCU, A., MIU, M., SIMION, M., IGNAT, T., BRAGARU, A., DUMITRU, L., TEODOSIU, G., *Gold and silver /Si nanocomposite layers*, Mat. Sci. and Eng., 2006, in press.